

A 23-Year Nationwide Study Revealing Aerosol-Driven Light Rain Shifts in China's Emission Control Era

Rou Zhang¹, Xiaoxiao Huang¹, Pu Wang¹, Guiquan Liu¹, Mengyu Liu¹, Songjian Zou¹, Lu Chen², Fang Zhang^{1*}

5 ¹School of Ecology and Environment, College of Artificial Intelligence, Harbin Institute of Technology (Shenzhen), Shenzhen 518055, China

²School of Urban and Planning, Yancheng Teachers University, Yancheng, 224051, China

Correspondence to: Fang Zhang (zhangfang2021@hit.edu.cn)

Abstract. Precipitation dynamics critically regulate Earth's hydrological cycle and climate system, yet

10 the mechanisms driving decadal-scale variations in light rain remain poorly quantified. Our analysis of a

23-year (2000–2022) national-scale dataset reveals contrasting trends in light precipitation occurrence: a

significant decline (1.0 days yr^{-1} , $p < 0.05$) during 2000–2013 followed by a pronounced increase (1.9 days yr^{-1} , $p < 0.01$) in 2013–2022. Cross-temporal analysis demonstrates a national wide inverse

5 correlation ($r = -0.55$, $p < 0.01$) between aerosol concentrations and light rain frequency in the China's

15 Emission Control Era, when the $\text{PM}_{2.5}$ shows an upward trajectory before 2013 followed by a markedly

downward decline thereafter, providing a natural experiment to quantify aerosol effects in precipitation.

Through multi-algorithm machine learning and causal inference modeling, we further identify aerosol-

cloud microphysical processes as the dominant driver, with $\text{PM}_{2.5}$ concentration changes explaining 59–

63% of the decadal trends of light rain. As a result, the $\text{PM}_{2.5}$ reduction (increase) enhances (reduces)

20 light rain frequency by $+1.97$ (-2.08) days yr^{-1} . Meteorological factors showed negligible temporal

variability and thus insignificant explanatory power (<10% for each individual factor) over a decadal

scale. Our findings establish, for the first time, the quantifiable aerosol microphysical effect on light

precipitation trends, highlighting dual benefits for China's emission control policies that $\text{PM}_{2.5}$ reduction

in 2013–2022 simultaneously enhanced light rain frequency while improving air quality. This work offers

25 critical insights for aligning air pollution mitigation with climate adaptation strategies.

1 Introduction

Precipitation serves as a pivotal physical process linking weather, climate, and the hydrological cycle.

Understanding the changes in precipitation and its influence mechanisms and factors are thus of great

significance. Light rain, a primary component of precipitation, is defined as precipitation with a daily

30 accumulation between 0.1 and 10 mm, following the China Meteorological Administration (CMA)

standard(Dunkerley, 2021). Despite its relatively low intensity, the cumulative amount of light rain still

accounts for a significant proportion of 20%~40% in total annual precipitation (Wang et al., 2021; Yuan

et al., 2024). In addition, light rain account for more than 70% of total number of rainy days, making a

significant contribution to effective precipitation in China (Fu et al., 2008; Qian et al., 2009a). Compared

35 to heavy precipitation, light rain can more easily infiltrate into the soil, and thereby plays a crucial role in

maintaining soil moisture, irrigating plants, and preventing forest fires(Trenberth et al., 2003). Previously,

the notable decrease in trace precipitation events or drizzle events during the years of 1950-2000 has

already manifested in China (Li et al., 2008; Qian et al., 2009b), In the context of climate change and

carbon emission reduction, the amount and frequency of light rain may change in China, thereby affecting

40 the climate and hydrological cycle.

In recent years, studies have analysed the characteristics and influencing factors of trends in light

rain changes in China based on long-term meteorological and aerosol dataset (Qian et al., 2009a; Jiang et

al. 2014; Ma et al., 2015). Research has shown that in most regions of China, particularly the eastern

regions, there has been a trend of decreasing light rain days and amounts since 1960, seasonal variations
45 have maintained the same trend as the annual average, with winter exhibiting more significant changes in
light rain days compared to other seasons (Huang and Wen, 2013; Ma et al., 2015; Wu, 2015; Zhang et
al., 2019). Although many studies have revealed the characteristics of long-term changes in light rain
days in China, it is still with big challenges to identify the driving factors. Some research have focused
on the analysing the relationship between long-term trends in meteorological factors or PM_{2.5}
50 concentrations and changes in light rain days (Fu and Dan, 2014; Wu et al., 2016; Bastin et al., 2019;
Zhang et al., 2019). Studies generally indicate that rising temperatures, increasing aerosol pollution, and
decreased relative humidity tend to suppress the occurrence of light rain (Fu and Dan, 2014; Zhou et al.,
2020; Luo et al., 2024). Lu et al. (2014) pointed out that variations and changes in rainfall total can be
dominated by changes in moisture and temperature. Studies have indicated that annual changes in the
55 number of light rain days are influenced mainly by changes in water vapor content over the eastern China
(Wu, 2015). However, it was pointed out that the correlation between large-scale water vapor transport
and light rain is not significant (Qian et al., 2009a). Statistical analysis also revealed positive correlations
between the light rain days and relative humidity (Wu et al., 2015; Zhang et al., 2019). Actually, the
decrease in relative humidity is primarily a result of rising temperature (Song et al., 2017; Zhou et al.,
60 2020). Some researchers argue that the increase in temperature reduces light rain days by affecting the
dew point temperature, as the air with the same water vapor content is more difficult to condense into
precipitation in a warmer environment than in a colder one (Qian et al., 2007). Huang et al. (Huang and
Wen, 2013; Huang et al., 2014) analysed the probable cause for the change of light rain events and
suggested that when atmospheric stability strengthens, it will promote an increase in light rain events,

65 whereas when atmospheric stability decreases, light rain events decrease. However, studies have also shown that stable atmospheric conditions are detrimental to the development of warm clouds, thereby suppressing the occurrence of light rain (Li et al., 2017).

In addition, some studies have focused on exploring the relationship between aerosol pollution and the number of light rainfall days. Aerosols can affect precipitation by serving as cloud condensation nuclei (known as Aerosol-Cloud Interactions, ACIs) or by altering the radiative energy budget of the atmosphere-earth system (Aerosol-Radiation Interactions, ARIs) (Ramanathan et al., 2001; Rosenfeld et al., 2008; Li et al., 2017). Research based on observational data suggests a negative correlation in the diurnal variation of aerosols concentration and light rainfall events due to Twomey effect (Choi et al., 2008; Fu and Dan, 2014). However, a study in the TengChong area found that while the number of light rainfall days showed a decreasing trend, visibility improved annually (Wu et al., 2016). Results from model simulations of aerosol effects indicate that light rainfall will decrease in heavily polluted areas, primarily due to the cloud microphysical effects of aerosols (Qian et al., 2009a; Wang et al., 2016; Shao et al., 2022), the atmospheric conditions with high aerosol loading can significantly increase the cloud droplet number concentration and reduce cloud droplet sizes compared to clean conditions. This can lead 75 to a significant decline in raindrop concentration and delay raindrop formation because smaller cloud droplets are less efficient in the collision and coalescence processes (Twomey, 1977; Qian et al., 2009a). Additionally, the increase in aerosol particles concentration has a significant impact on precipitation in China due to the aerosol radiation effect. Fan et al. (2015) found that the light rainfall was significantly suppressed in the southwestern region of China based on WRF-Chem simulation. They further showed 80

85 that this is may be attributed to the weakening of near-surface shortwave radiation by the aerosol radiation effect, which enhances tropospheric stability and reduces the occurrence of precipitation (Liu et al., 2022).

Overall, there remains significant uncertainty regarding the mechanisms influencing the occurrence of light rain. Most previous studies have primarily focused on the analysis of a single or very limited factors, and the relative importance of various influencing factors to the light rainfall was mostly 90 qualitatively assessed, lacking a quantitative and comprehensive evaluation. Additionally, studies on light rain days often limited to time periods when the aerosol pollution was continuously intensified in China, e.g. from around 1960s to around 2010s. A comprehensive investigation on the changes of light rainfall frequency in the most recent years of China's emission control era and its driving factors has not yet been conducted. Given the significant changes in PM_{2.5} pollution in China before and after stringent emission 95 reduction measures, as well as the background of intensified global warming and increasing number of extreme weather events, the trends and influencing factors of the light rain may undergo changes. Therefore, this study aims to obtain insights on the mechanisms affecting the changes of light rainfall days over China by combining multi datasets, multi-algorithm machine learning and causal inference modeling. The study period has been focused on the years of 2000-2022, a period during which PM_{2.5} 100 concentrations show a significant upward trajectory before 2013 followed by a markedly downward decline thereafter (see Section 3.1), providing a natural experiment to quantify aerosol effects in precipitation. Section 2 presents the methods and data; In Section 3.1, we present the long-term variations in the light rain frequency as well as the influencing factors over the studied period. In Section 3.2 & 3.3, we utilize the machine learning techniques (XGBoost and SHapley Additive exPlanations, SHAP) to 105 quantify the importance of each individual factor to the occurrence of light rain. In Section 3.4, we

discussed the key factors driving the long-term trends of the light rain frequency during the two periods. We finally incorporate Structural Equation Model (SEM) to derive insights on physical mechanisms and interactions between the various factors and the light rain occurrence.

2 Data and Methods

110 2.1 Data

In this study, the frequency of number of light rain days was calculated based on the dataset of CPC Global Unified Gauge-Based Analysis of Daily Precipitation (CPC-Global) (<https://psl.noaa.gov/data/global/data.cpc.globalprecip.html>). The CPC-Global dataset is with a spatial resolution of $0.5^\circ \times 0.5^\circ$ and produced based on assimilation and interpolation of observations from 30,000 stations by National Oceanic and Atmospheric Administration (NOAA) through the CPC Unified Precipitation Project (Xie et al., 2010). The daily ERA5 reanalysis data from 2000 to 2022 provided by the European Centre for Medium-range Weather Forecasts (ECMWF) was also used in this study (<https://cds.climate.copernicus.eu/>). These data include the relative humidity (RH) at 850 hpa, temperature (T) at 2 m height, the wind speed (WS) at 850 hpa, total column cloud liquid water (TCLW), low cloud cover (LCC), convective available potential energy (CAPE) and evaporation (E). The horizontal resolution for the meteorological data is $0.25^\circ \times 0.25^\circ$. The PM_{2.5} data are obtained from the China High Air Pollutants dataset (CHAP) at a spatial resolution of 1 km \times 1 km from 2000 to 2022 (Wei et al., 2021, 2019; Wei, 2024).

2.2 Methods

In this study We defined the light rain event as the daily precipitation is between 0.1 and 10 mm
125 (Qian et al., 2009b; Huang and Wen, 2013; Wu et al., 2015) which is referenced from the standards of the
CMA.

To better demonstrate the effect of changes in PM_{2.5} and other meteorological parameters on changes
of the number of light rain days, we conducted the following-analysis using data based on two periods
from 2000 to 2013 and from 2013 to 2022these two periods. The year 2013 was selected as the breakpoint
130 because it marks a definitive shift in China's air pollution policy with the implementation of the national
"Air Pollution Prevention and Control Action Plan", which led to a proven reversal in the long-term trend
of PM_{2.5} concentrations nationwide (Wei et al., 2021). Moreover, the frequency of light rain in most
regions of China, especially those heavily affected by human activities, also showed a change pattern of
first decreasing and then increasing before and after 2013 (Fig. 1, Fig. 2). The XGBoost model was
135 applied separately to the two periods (2000 – 2013 and 2013 – 2022) rather than to the entire dataset. This
approach was chosen because the underlying physical relationships between the predictors and light rain
are expected to differ significantly between the pollution-accumulating and pollution-abatement regimes.
Training separate models prevents the estimation of a misleading "average" relationship and allows for a
more accurate quantification of the distinct drivers operative in each period. Least squares technique
140 (linear regression) is firstly employed to estimate the annual trends of light rain days and the examined
factors. Additionally, the extreme gradient boosting (XGBoost) model is applied to examine the impact
of these factors, including PM_{2.5}, RH, WS, T, E, TCLW, CAPE, and LCC, on the number of light rain
days. The selection of these specific factors is grounded in their well-established physical linkages to light

rain processes, as extensively documented in prior studies (Qian et al., 2009a; Huang and Wen, 2013; Li 145 et al., 2017). Briefly, $PM_{2.5}$ is included to quantify aerosol impacts on cloud microphysics, while the meteorological variables collectively represent the thermodynamic, moisture, dynamic, and cloud-related conditions that are fundamental to light rain formation. This approach ensures our model captures the key mechanistic drivers identified in the literature.

The importance of each parameter affecting the accuracy of the light rain days prediction is assessed. 150 The XGBoost model, which is a powerful and reliable machine learning technique, optimizes the gradient boosted decision tree algorithm to solve regression and classification problems (Chen and Guestrin, 2016). It offers several advantages, such as handling missing values, preventing overfitting, enhancing computing speed and accuracy, and has been widely applied in predicting air pollutants and emissions (Gui et al., 2020; Si and Du, 2020, 2020). Previous studies have shown that XGBoost performs well with 155 relatively small-scale datasets (Cheng et al., 2021; 2023). This work used 5-fold cross-validation of the training set to test the performance of the XGBoost model and defined the parameter search space to determine the optimal model parameters, finally generating the prediction results. The predicted frequency of the number of light rain days by the XGBoost method exhibit high consistency with the observed values, with mean R^2 of 0.83 and 0.90 (Fig. S3). Through K-fold cross-validation evaluation, 160 each model achieved a mean coefficient of determination (R^2) of 0.80 on the cross-regional dataset, demonstrating robust generalization performance across different geospatial scales. Then, the drivers of the long-term variations of the light rain days over the two periods were further explored. For this, the annual trend (depicted by slope obtained based on linear fitting) of daily data for each individual factor as well as the frequency of light rain days were firstly calculated as the input variables and target

165 parameter respectively. The result shows good performance with mean R^2 of 0.90 (Fig. S6), The K-fold cross-validation ($R^2 > 0.88$) results also demonstrate robust performance across different datasets.

SHAP is a machine learning interpretability technique based on coalitional game theory (Lundberg and Lee, 2017), with its core mechanism lying in the mathematical quantification of feature contributions. Within the SHAP framework, SHAP values essentially represent a formalized mathematical deformation 170 of Shapley values, which decompose model predictions to attribute the deviation of each sample's predicted outcome to the contributions of individual features. The explanation could be specified as:

$$g(z') = \phi_0 + \sum_j^M \phi_j z'_j g$$

175 where g is the explanation model, $z' \in \{0,1\}^M$ is the simplified features, M is the maximum coalition size, and $\phi_j \in R$ is the weighted average of all marginal contributions for a predictor variable j , the Shapley values.

This method is particularly effective for identifying the relative importance of predictor variables in XGBoost models, providing feature attribution analysis that integrates global consistency with local 180 interpretability. Compared to feature importance methods such as the gain method or split count, SHAP not only reveals key driving factors through global importance rankings but also visualizes feature contribution distributions at the individual sample level, enabling an interpretability analysis of the interaction between model prediction and characteristic effect.

SEM is a method that is usually used to test hypotheses on relationships of multi factors within a complex system (Lamb et al., 2014; Ganjurjav et al., 2021). These hypotheses are articulated in the form 185 of a series of regression equations, known as structural equations. This model enables the simultaneous analysis of multiple variables with causal relationships and overcomes the limitations of traditional

multivariate analytical techniques such as multivariate analysis of variance and correlation analysis. One of the most important advantages of SEM is its capacity to disentangle complex interdependencies among multiple parameters. This is achieved by estimating the independent (direct) effect of each variable while simultaneously accounting for its correlations with other variables in the model.

When constructing an SEM, hypotheses about causal relationships between variables are first formulated based on theoretical and prior research findings, and then the result is adjusted according to whether the fit indices meet statistical criteria. The key indices for evaluating SEM model fit include the Comparative Fit Index (CFI), Root Mean Square Error of Approximation (RMSEA), and Standardized Root Mean Square Residual (SRMR). In general, when CFI approaches 1, $0 \leq \text{RMSEA} \leq 0.05$, and $0 \leq \text{SRMR} \leq 0.08$, the model indicates a very good fit (Schreiber et al., 2006, Ma et al., 2022). In addition, the chi-square test (χ^2) and Adjusted Goodness of Fit Index (AGFI) are also commonly used for model evaluation. In this study, the final model fitting results showed that CFI was 0.998 and RMSEA was 0.033, which indicates that the SEM had a very good fit with the data and that the model fit was almost ideal.

200 **3 Results**

3.1 Nationwide inverse correlation of long-term changes between aerosol concentrations and light rain frequency

Figure 1 illustrates the spatial distributions and long-term trends of light precipitation frequency and PM_{2.5} mass concentrations across China during the studied periods (2000 – 2022). Statistically significant decreasing trends in light rain days (mean rate: 1.0 days yr⁻¹, $p < 0.05$) were observed nationwide during

2000 – 2013, with the most pronounced decline in southern China (2.3 days yr^{-1} , $p < 0.01$) (Fig. 1).

Conversely, a reversal trend emerged during 2013 – 2022, showing continent-wide increases (1.9 days yr^{-1} , $p < 0.01$), particularly in southwestern China and the Yangtze River Basin (central-eastern regions), where the growth rate reached 2.6 days yr^{-1} . The data analysis also reveals an inverse correlation between

210 light precipitation trends and $\text{PM}_{2.5}$ variations: a substantial significant $\text{PM}_{2.5}$ increase ($0.39 \mu\text{g m}^{-3} \text{yr}^{-1}$, $p < 0.01$) occurred during 2000 – 2013, contrasting with a substantial-significant decline ($2.5 \mu\text{g m}^{-3} \text{yr}^{-1}$, $p < 0.01$) post - 2013. Actually, the rapid decrease in $\text{PM}_{2.5}$ mass concentration since 2013 have been widely observed due to the implementation of the national “Air Pollution Prevention and Control Action Plan” in China (Zhang et al., 2020; Wei et al., 2021; Bai et al., 2024; Zhang et al., 2024). Note that, before
215 2013, the national average annual light rain days showed significant interannual fluctuations, with the
lowest number of light rain days recorded in 2007 (Fig. 1a). This makes it seem as if 2007 was a turning
point where the trend of light rain frequency shifted from decreasing to increasing. However, when the
analysis is focused on specific different regions, it is found that the turning point of light rain frequency
still occurred in 2013 (Fig. 2). Considering the variation trend of $\text{PM}_{2.5}$ comprehensively, this study
220 divides the research period into two phases of 2001–2013 and 2013–2022.

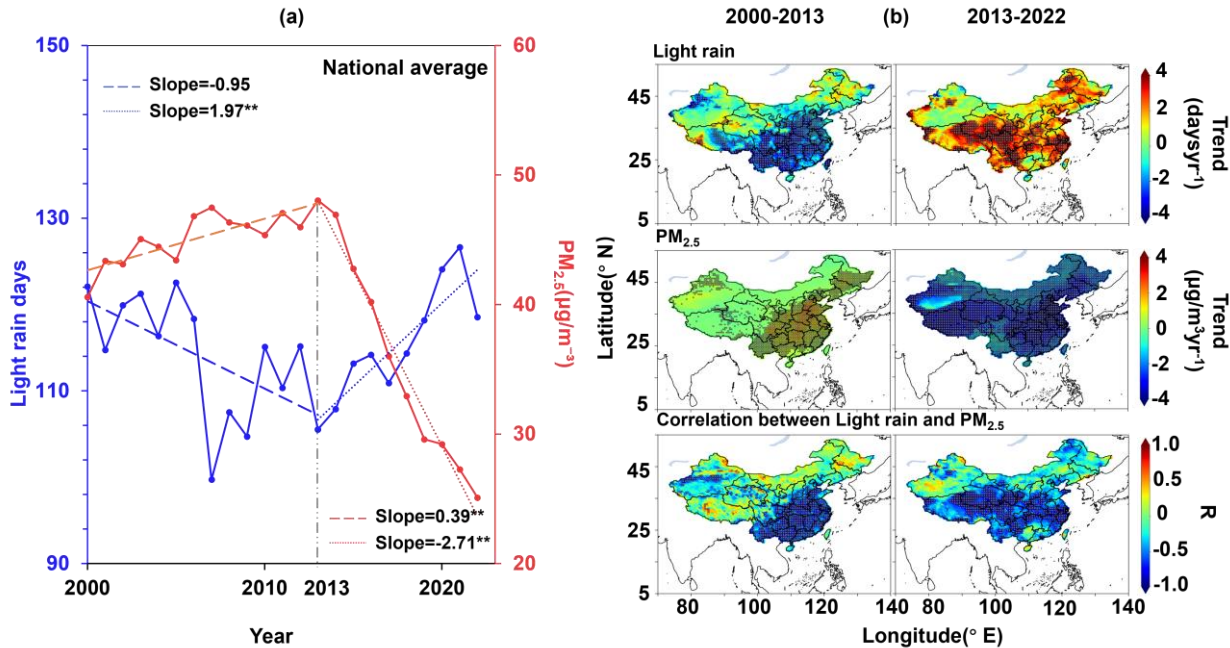


Figure 1. Nationally averaged time series of light rain days (blue lines) and PM_{2.5} mass concentration (red lines) from 2000 to 2022. The dashed lines represent the piecewise linear trends for the periods 2000–2013 and 2013–2022, with the slopes indicated. Trends significant at the 95% confidence level are marked with **. (b) Spatial distribution of the trends of light rain, PM_{2.5} and spatial correlation between PM_{2.5} and light rain days in 2000–2013 and 2013–2022. This map of China is created based on same-origin data provided by the Tianditu Platform (www.tianditu.gov.cn). (black dots indicate passing the 95% significance test).

In particular, this inverse relationship is most evident in six anthropogenically influenced regions (Fig. 2): North China (NC), South China (SC), East China (EC), Southwest China (SWC), Central-South China (CSC), and the Fenwei Plain (FW). This regional division is based on established frameworks that consider distinct physiographic (e.g., topographic basins, climate zones) and anthropogenic (e.g.,

population density, industrial activity) characteristics (Chen et al., 2024). For instance, the Fenwei Plain

235 (FW) is treated separately from North China (NC) due to its unique enclosed topography that fosters pollution accumulation, despite some similarities in overall trends.

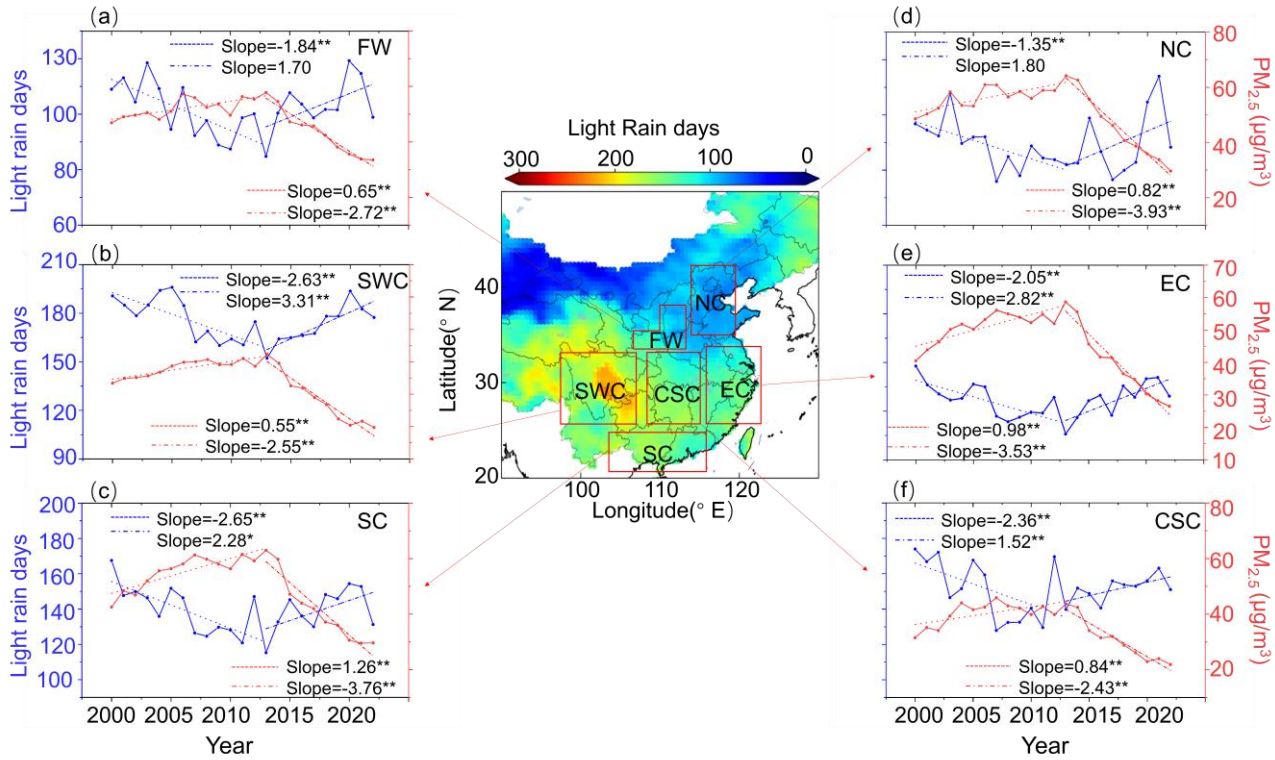


Figure 2. The fitted variation trends of light rain days (blue lines) and the fitted variation trends of PM_{2.5}

(red lines) in different six selected regions. The middle map shows the spatial distribution of average light

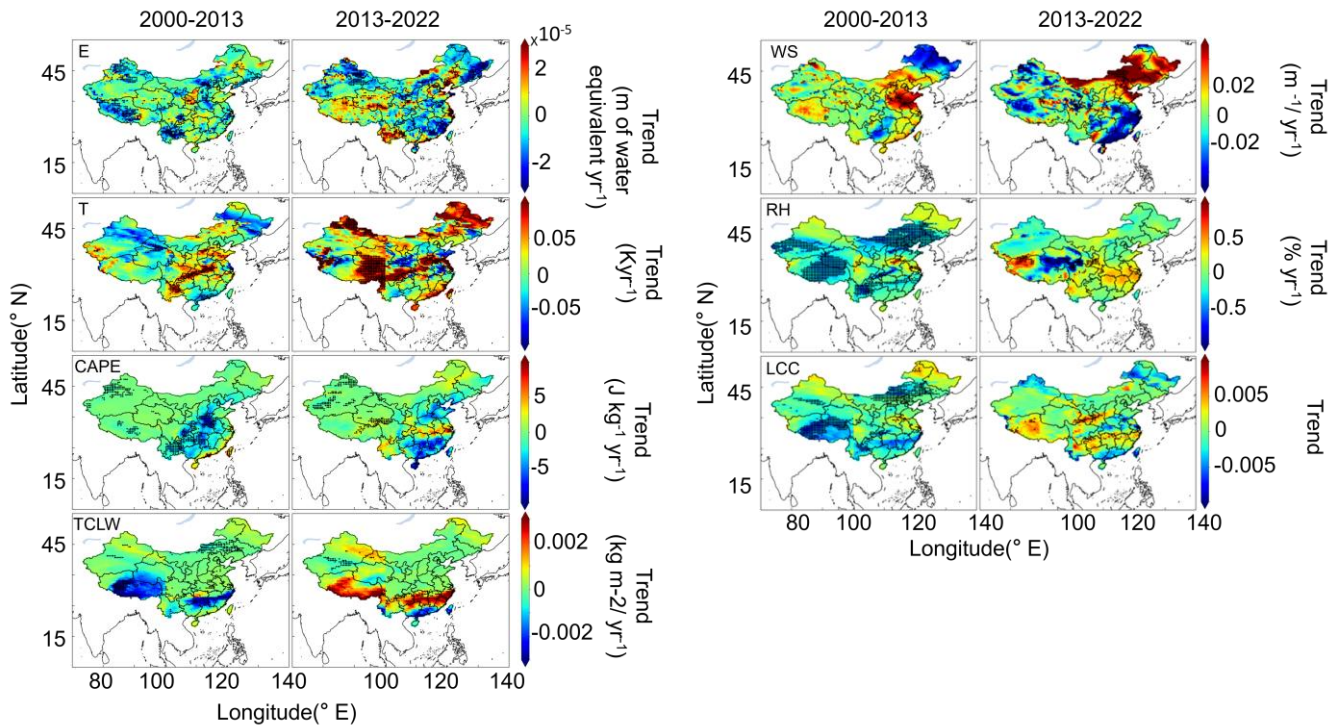
240 rain days during 2000–2022 and the six selected study regions.

Since previous studies attribute light rain suppression in polluted regions to aerosol-cloud microphysical interactions (Qian et al., 2009b; Wang et al., 2016; Shao et al., 2022), our analysis suggests that the observed decadal shifts in light precipitation (2000 – 2013 decline vs. 2013 – 2022 increase) are likely driven by long-term aerosol concentration variability. Notably, regions with minimal anthropogenic

245 activities (e.g., Inner Mongolia and northwestern China) exhibited no significant PM_{2.5}-light rain correlations but with good correlations with meteorological factors (e.g., RH) (Fig. 1, Fig. S2), implying contributions from non-aerosol factors.

Figure 3 depicts the long-term trends of meteorological factors (T, RH, CAPE, E, LCC, TCLW, and WS) potentially associated with light rain variability in China during 2000 – 2013 and 2013 – 2022, while 250 the statistical significance ($p < 0.05$) of these trends is shown in Supplementary Fig. S1. A key observation is that, in contrast to the strong and statistically significant nationwide trends seen in PM_{2.5}, the trends of these meteorological parameters are characterized by pronounced spatial heterogeneity and largely insignificant changes over large portions of China. For the E, from 2000 to 2013, approximately 60% of regions exhibited insignificant trends, only with the significant decline ($p < 0.05$) observed in 255 southwestern China and the Qinghai-Tibet Plateau (Fig. S2). During 2013 – 2022, E just decreased significantly in very few areas of northeastern China and northern Xinjiang, areas concurrent with RH increases (Cong et al., 2009). Conversely, large areas of southeastern China experienced nonsignificant E reductions. Notably, E-enhanced regions seems expanded in recent decades, likely attributable to global warming effects (IPCC, 2021). However, the enhanment is not statistically significant (Fig. S2). Analysis 260 reveals that 56% of Chinese regions showed T increases slightly during 2000 – 2013, with accelerated warming rates post - 2013. The CAPE demonstrated weakened trends across southeastern China during 2000 – 2013, while remaining stable in western/northwestern regions. This spatial pattern aligns with anthropogenic aerosol impacts. The aggravated aerosol pollution over 2000 - 2013 likely suppressed convection in densely populated eastern China via microphysical mechanisms (Zhao et al., 2006). 265 However, PM_{2.5} reductions since 2013 moderated CAPE declines, with some regions (e.g., middle-lower

Yangtze River) even exhibiting strengthening trends, indicating meteorological sensitivity to aerosol loading changes. The TCLW decreased only in the Yangtze River Basin and Tibetan Plateau during 2000 – 2013, but reversed to increasing trends post - 2013. There are no evident variations (statistically insignificant) in TCLW elsewhere during the two periods (Fig. S2). Nationwide WS reductions 270 (statistically nonsignificant) were observed during both periods, though southeastern China experienced accelerated declines post - 2013, potentially linked to persistent particulate pollution and urbanization processes (Zhang and Wang, 2021). The RH declines affected less than 30% of China during 2000 – 2013, most prominently in the Tibetan Plateau, northeastern/southwestern China. During 2013 – 2022, it is observed with nonsignificant RH variations becoming dominant nationwide. The LCC trends spatially 275 mirrored RH patterns, likely underscoring their coupled responses to anthropogenic and climatic drivers. While these meteorological parameters exhibited spatially variable trends, their magnitudes were generally much smaller than PM_{2.5} variations. Subsequent sections will quantitatively evaluate their combined impacts on light rain frequency.

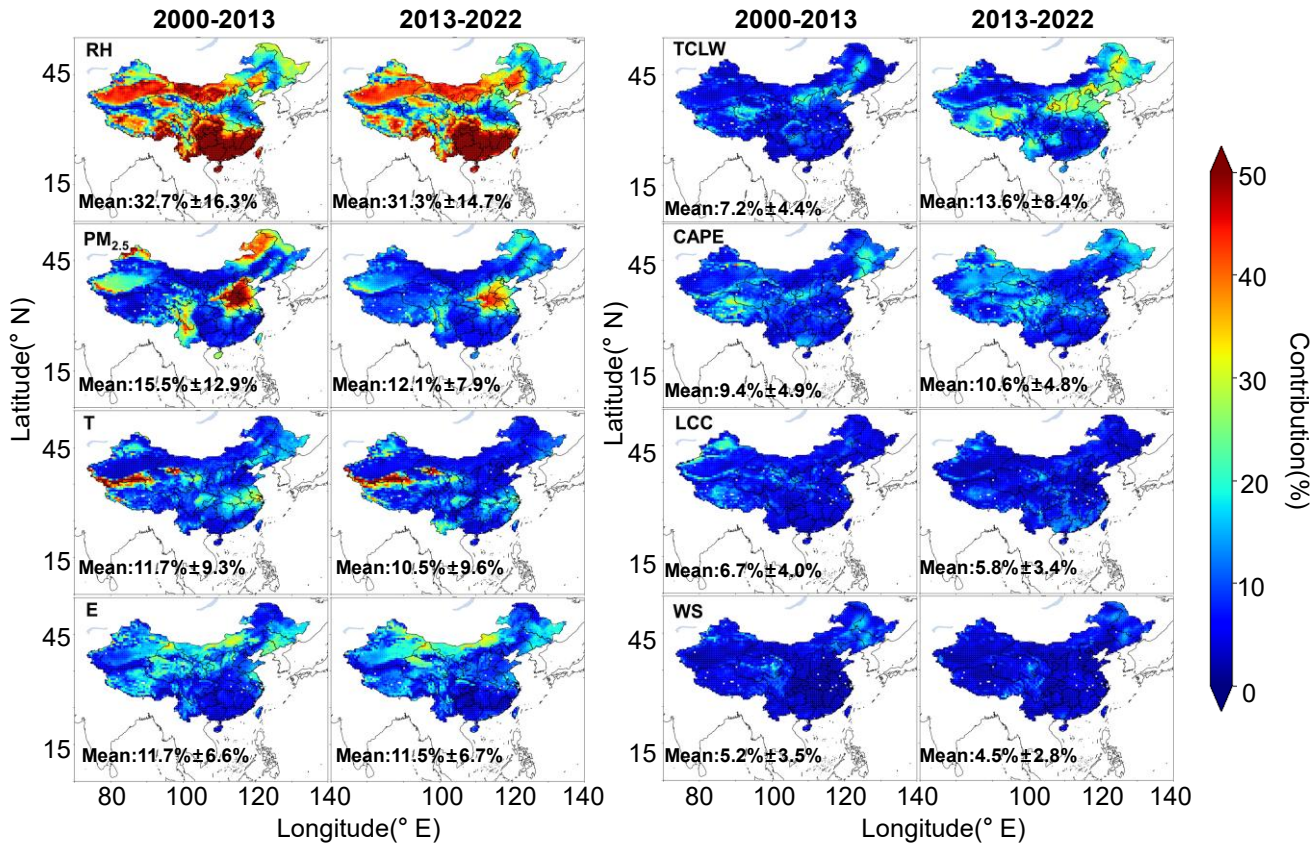


280 **Figure 3.** The fitted variation trends of other affecting factors of E, T, CAPE, TCLW, WS RH, and LCC of China over 2000 - 2013 and 2013 - 2022.

3.2 Quantifying the relative contributions of individual factors to light precipitation events

To elucidate the influence of aerosols and meteorological parameters on light precipitation events, variable importance metrics were derived using the machine learning - based XGBoost algorithm. 285 Considering that the temporal variation trends of these factors are not identical, we presented and analyzed the conditions of the two research periods (2000–2013 and 2013–2022) (Fig. 4) – this was done to compare and explore whether the relative contribution or importance of each factor to precipitation has changed across different stages. The XGBoost-based model demonstrates robust predictive capability, achieving a correlation coefficient of 0.83 and 0.90 (Slope: 0.80, 0.85 $p < 0.01$) between predicted and

290 observed light precipitation events (Fig. S3). This validation ensures the reliability of subsequent
parameter importance evaluations for elucidating meteorological drivers of light rain. Figure 4 quantifies
the relative contributions of the PM_{2.5} and meteorological factors (RH, T, E, TCLW, CAPE, LCC, WS)
to light rain occurrence during 2000 – 2013 and 2013 – 2022. Nationwide, RH exerted the dominant
influence, accounting for 32% of light rain variability across both periods. The PM_{2.5}, T, and E followed
295 as key drivers, with mean contributions of 15.5%/11.7%/11.7% in 2000 – 2013 and 12.1%/10.5%/11.5%
in 2013 – 2022 respectively. Notably, the contribution of PM_{2.5} declined from 15.5% to 12.1% (a 3.4%
decrease, $p < 0.05$), coinciding with China's stringent emission controls (Shao et al., 2022; Wang et al.,
2016). Conversely, the contributions of TCLW and CAPE increased significantly from 7.2%/9.4% in
2000 – 2013 to 13.6%/10.6% in 2013 – 2022 ($p < 0.01$). LCC and WS remained negligibly minor factors
300 (< 6% contribution). Moreover, spatial heterogeneity (Fig. 3) revealed no substantial differences in factor
contributions between the two periods, except for PM_{2.5} and TCLW. Conspicuously, the meteorological
factors exhibited statistically insignificant temporal trends, implying stable physical mechanisms
underlying their impacts on light rain.



305 **Figure 4.** The relative contribution of RH, PM_{2.5} mass concentration, T, E, TCLW, CAPE, LCC and WS to light rain events over 2000 - 2013 and 2013 - 2022.

Spatial heterogeneity characterizes the relative importance of meteorological factors (Fig. 5). For instance, the RH exerts critical influence in southeastern and northwestern China, peaking at 50% contribution in southern regions. This spatial pattern aligns with established findings showing significant 310 RH - light rain day correlations in southern China (Wu et al., 2015; S. Zhang et al., 2019; Zhou et al., 2020). Conversely, the contribution of RH diminishes to ~10% in northern regions, likely attributable to lower atmospheric moisture content (Fig. 5b). In contrast, PM_{2.5} emerges as the dominant driver in northern China, especially in North China Plain (NCP), where aerosol concentrations exceed those in

pristine western regions (Fig. S4). This aerosol-mediated regulation aligns with cloud microphysical

315 mechanisms suppressing light precipitation (Qian et al., 2009b; Yang et al., 2016). The E demonstrates pronounced influence in arid Inner Mongolia and northwestern China, consistent with hydrological sensitivity in water - limited ecosystems (Chen Yaning et al., 2014; Yang Yaqing et al., 2024). The E - light rain relationship weakens eastward, reflecting enhanced soil moisture buffering in humid regions.

320 The TCLW assumes greater significance in western and northeastern China, where the water vapor content is relatively low, the warm cloud precipitation process, which relies on the growth of liquid water and the collision and coalescence of water droplets, makes the TCLW a crucial factor for the occurrence of light rain (Gao et al., 2016). Notably, importance of TCLW increased significantly (+ 18%) in NCP and northeastern China post - 2013, coinciding with PM_{2.5} reductions that reduced cloud condensation nuclei (CCN) and elevated cloud droplet coalescence efficiency (Twomey, 1977; Guo et al., 2019).

325 Consequently, even small changes in TCLW can directly reflect the occurrence of light rain. These findings underscore the complexity of regional meteorological controls, necessitating regionalized analyses for mechanistic correlation.

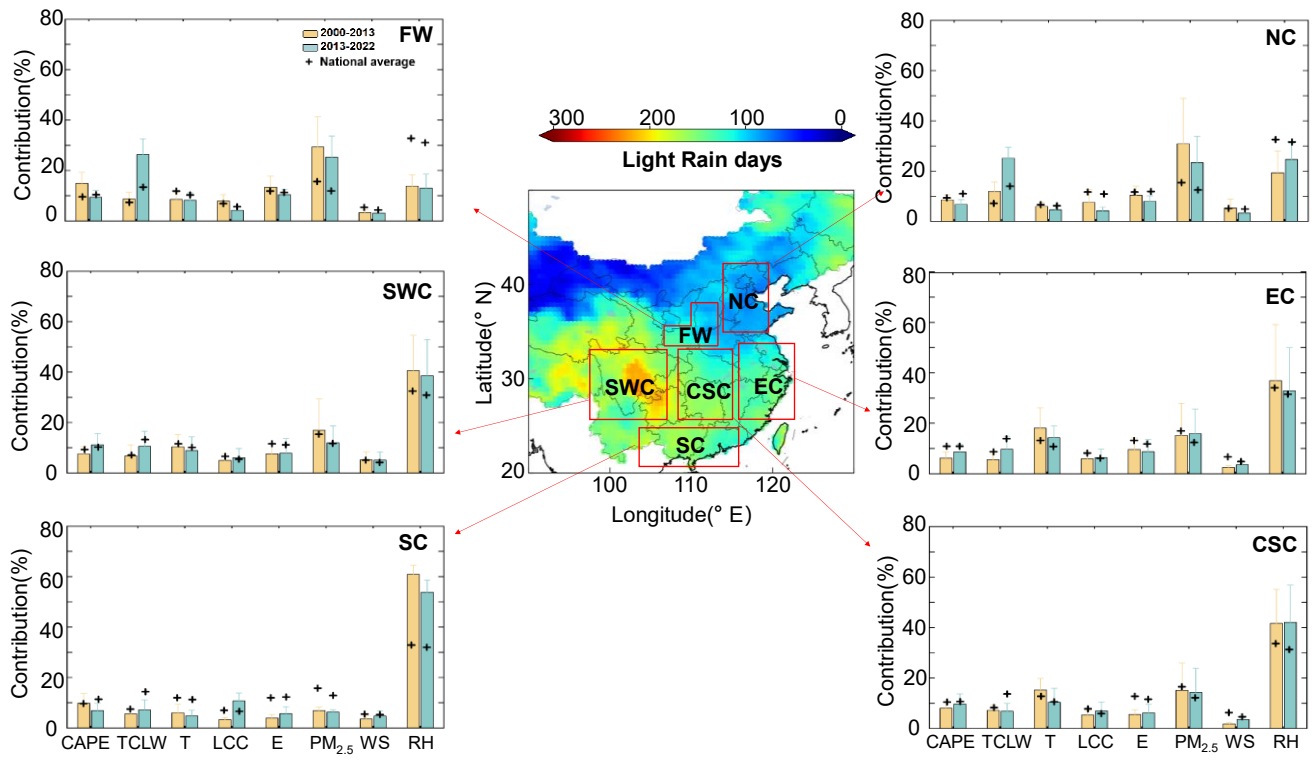


Figure 5. Comparison of the contribution of individual factors to light rain events over 2000 - 2013 and

330 2013 - 2022 in the selected six regions of China.

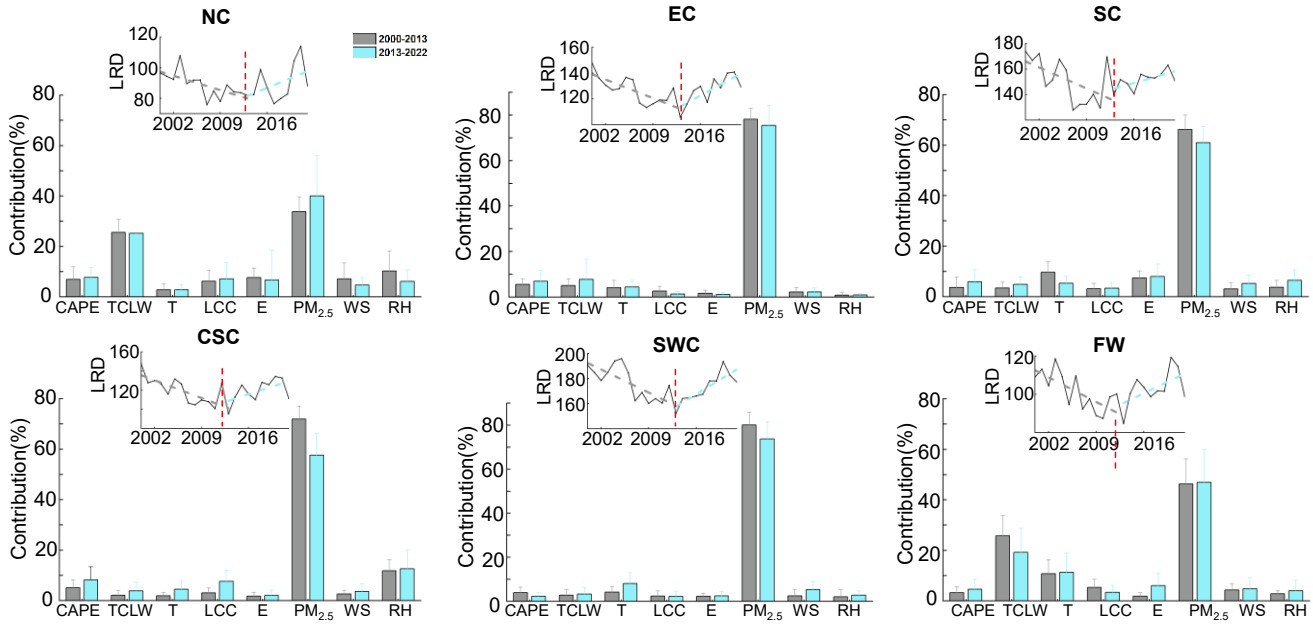
3.3 Comparison of the relative contributions of individual factors to light precipitation events in selected regions of China

The analysis is further conducted in the six typical areas with elevated anthropogenic emissions. As shown in Fig. 5, there are large differences in the dominant factors affecting light rain frequency across 335 regions. The RH plays a leading role in SC, EC, SWC, and CSC regions, with mean contributions of ~40%. In FW and NC regions, RH contributions diminish to 15–20%, whereas PM_{2.5} contributions increase markedly (20–30%), exceeding the national average by approximately twofold. This anthropogenic imprint is amplified in other high-emission regions (CSC, SWC, EC), where PM_{2.5} exhibits

considerable influence. Other factors (CAPE, WS, T, E, LCC) show no substantial variations in
340 contributions (< 10%) across the six regions. These findings indicate the dominant role of anthropogenic emissions in light rain occurrence within heavily polluted areas. Notably, impact of PM_{2.5} declined slightly in NC and FW during 2013 – 2022 compared to 2000 – 2013, aligning with China's pollution controls. The declines are consistent with decreases in the national average but showing steeper reductions. Concurrently, TCLW gained prominence in most regions (except CSC) post - 2013, increasing its
345 contribution to near 30%. These results underscore aerosol-cloud microphysical effects as critical regulators of light precipitation in polluted regions.

3.4 Factors and mechanisms that drive the long-term trends of light rain frequency

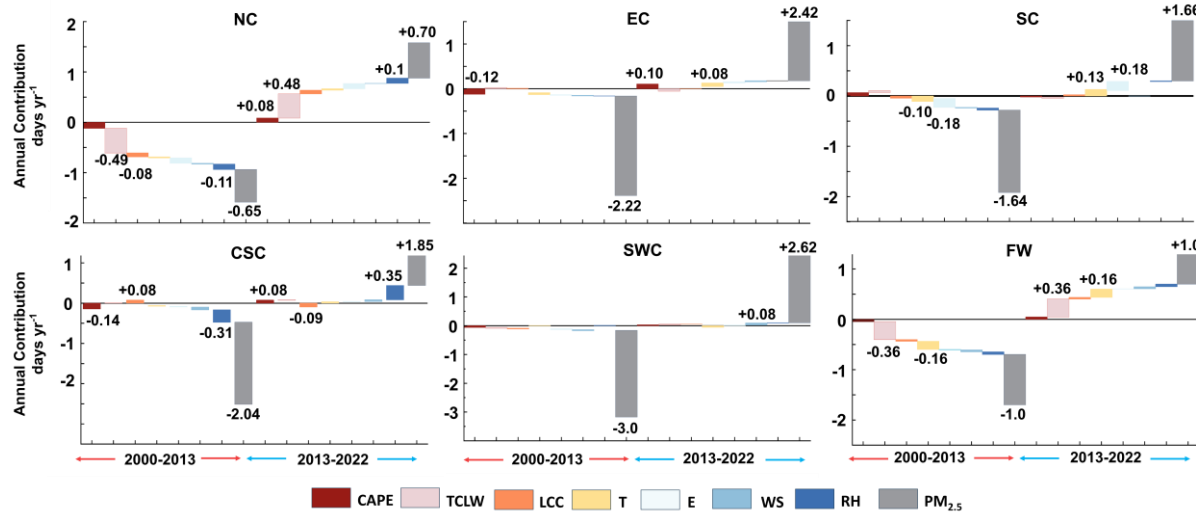
To elucidate the drivers of long-term trends in light rain day frequency described in Section 3.1, we systematically investigated the relative contributions of multi-factors using an integrated machine
350 learning (XGBoost), interpretability technique (SHAP) and SEM framework (Fig. 6). As stated previously, considering that the temporal variation trends of these factors are not identical, we presented and analysed the conditions of the two research periods (2000–2013 and 2013–2022) – this was done to compare and explore whether the driving factors of influencing the precipitation long-term trends has changed across different stages. Therefore, this dual-method approach quantifies both observed patterns (e.g., downward
355 trends in 2000–2013 vs. upward trends post - 2013) and underlying causal mechanisms. The results show good performance of our established model for predicting the trends of light rain frequency (with correlation coefficient R²=0.90 between the measured and predicted trends of light rain frequency) (Fig. S5).



360 **Figure 6.** Factors that drive the long-term trends of light rain frequency in the selected six regions of China. The small graphs embedded in the middle are the average trends of light rain frequency over 2000 - 2022 in the six regions, and the grey lines represent the fitted trend of light rain days from 2000 to 2013, while the blue lines depict the fitted trend for the period of 2013 - 2022.

365 The results demonstrate aerosol dominant role in driving long-term trends in light precipitation frequency across both periods, contributing 59–63% to the interannual variability of annual light rain days (Fig. 6). Specifically, the increasing trend in PM_{2.5} concentrations in 2000 - 2013 has led to varying magnitudes of decreases in the number of light rain days in the six regions, 0.65 days yr⁻¹ (NC), 2.22 days yr⁻¹ (EC), 1.64 days yr⁻¹ (SC), 2.04 days yr⁻¹ (CSC), 3.0 days yr⁻¹ (SWC), and 1.0 days yr⁻¹ (FW). (Fig. 7). Conversely, the pronounced decrease in PM_{2.5} levels from 2013 to 2022 has increased the light rain days of 0.7 days yr⁻¹ (NC), 2.42 days yr⁻¹ (EC), 1.66 days yr⁻¹ (SC), 1.85 days yr⁻¹ (CSC), 2.62 days yr⁻¹ (SWC), and 1.0 days yr⁻¹ (FW) (Fig. 7). Note that, compared to the period of 2000 - 2013, the relative

importance of the variations in PM_{2.5} in affecting the light rain in recent years of 2013 - 2022 becomes more prominent likely associated with the rapid nationwide decrease of aerosol concentrations since 2013. This aligns with Twomey's cloud albedo effect (Twomey, 1977), where elevated aerosol loadings 375 suppress light precipitation via cloud microphysical feedbacks (Qian et al., 2009b; Wang et al., 2016; Shao et al., 2022). Reduced aerosol concentrations post - 2013 attenuated these suppression effects, enhancing light rain frequency through improved cloud droplet coalescence efficiency. Machine learning-based analysis further elucidates this underlying microphysical aerosol-mediated mechanism (Figs. 6,7), revealing aerosols dominant influence on light precipitation. These findings reconcile national-scale 380 aerosol-light rain described in Section 3.1 with microphysical process dynamics. Averaging the regional results from Fig. 7, the national mean contribution of PM_{2.5} was -2.08 days yr⁻¹ during 2000-2013 and +1.97 days yr⁻¹ during 2013-2022.



385 **Figure 7.** Quantified contribution of each factor to the long-term changes of light rain days in the six selected regions of China over the periods of 2000 - 2013 and 2013 - 2022.

Other meteorological factors, such as RH and LCC, demonstrated significant positive correlations with light rain day frequency in most regions (Figs. S7-11). Our trend analysis in Section 3.1 revealed that they, along with the new insights from regional analysis (Fig. 8), exhibited statistically insignificant long-term changes over the study period. Consequently, their quantified contributions to interannual variability
390 were negligible (<10%), further supporting the conclusion that aerosols were the dominant driver of the observed trend reversal. Notably, in NC, the TCLW showed considerable importance in regulating the long-term variations of light rain frequency, explaining 26% of light rain days decline (about - 0.49 days yr^{-1}) over 2000 - 2013 and 25% of the light rain increase (about + 0.48 days yr^{-1}) during 2013 - 2022. Similar patterns were observed in FW, likely attributable to shared climatic and pollution regimes between
395 these two northern regions.

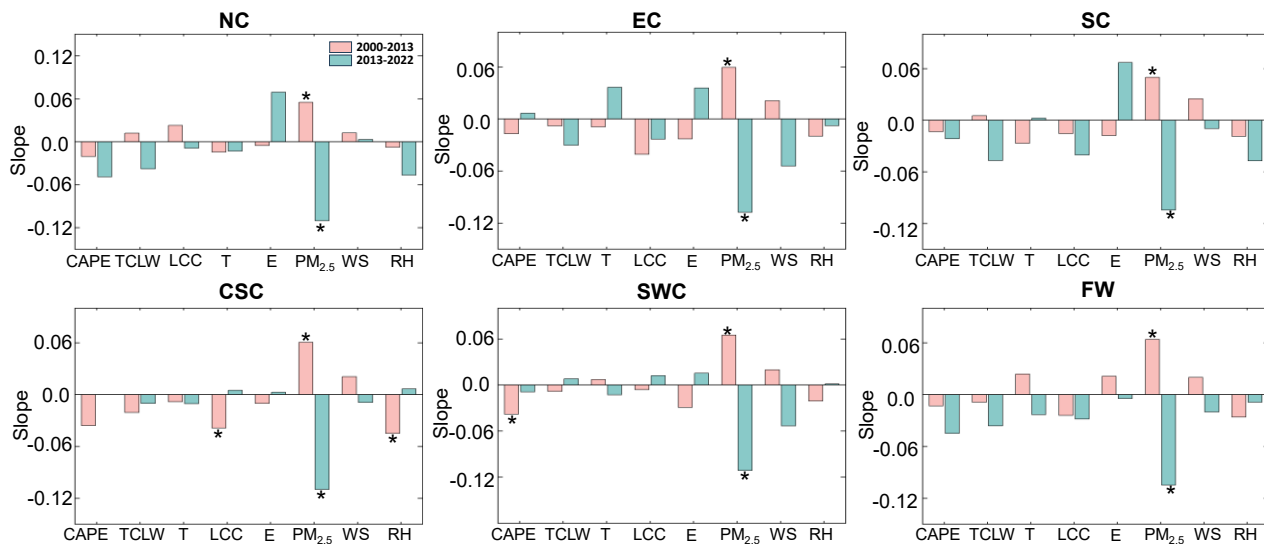
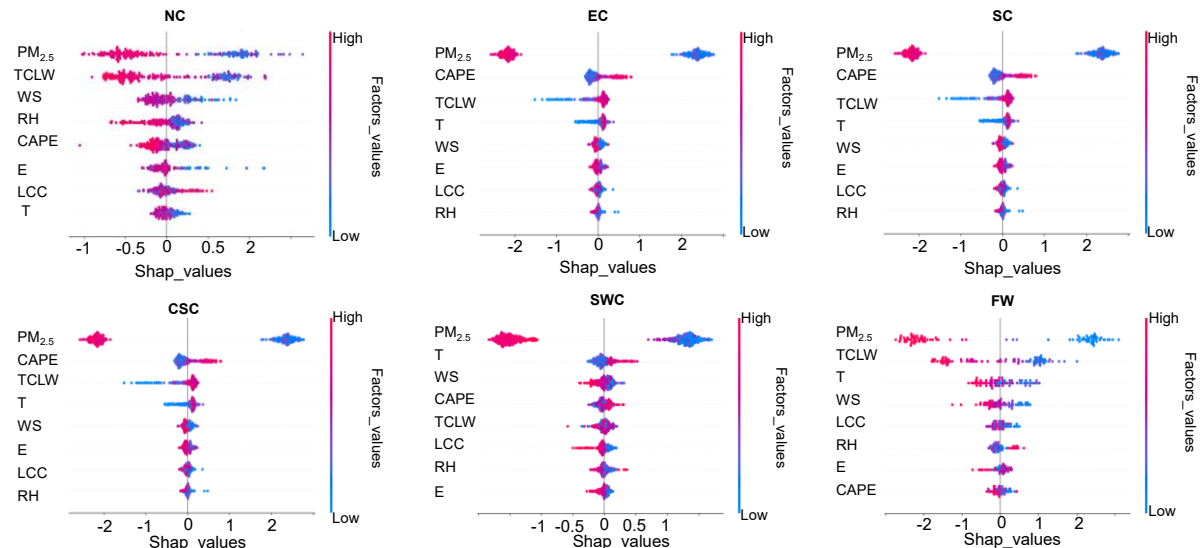


Figure 8. The regional average long-term trends of each individual factor in the selected six regions of China. The black asterisk (*) represent the fitted trend that passes the significance test.

4 Discussion and conclusion

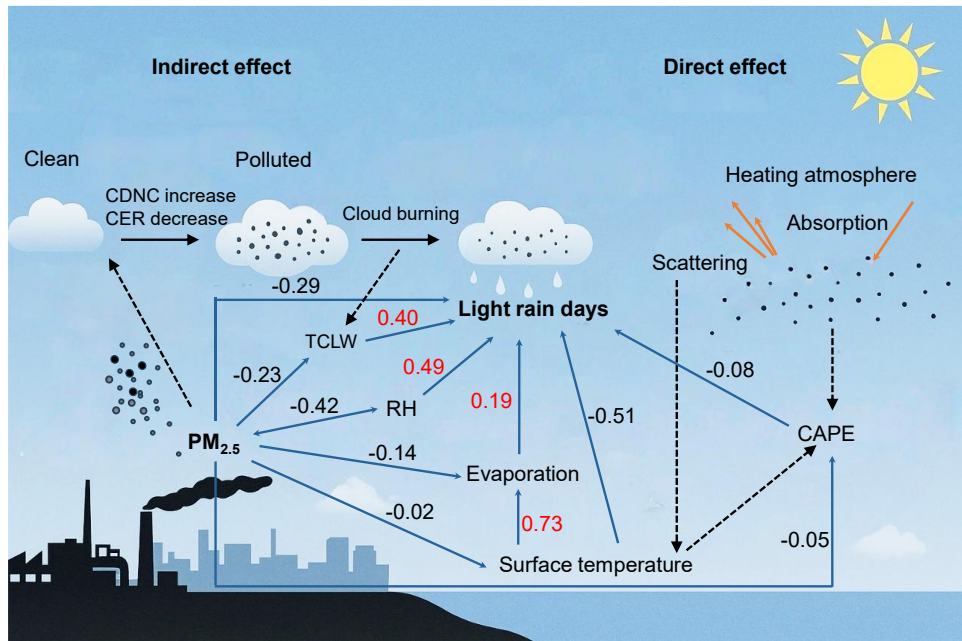
400 To systematically validate our findings, we conducted supplementary analyses using SHAP and SEM (Figs. 9-10). Results consistently demonstrate that PM_{2.5} long-term trends exert the most critical influence on light rain day variability across the six regions. Notably, negative SHAP values (−0.40 to −3.82, depending on regional variations) emerge under elevated PM_{2.5} concentrations (>40 $\mu\text{g m}^{-3}$), indicating aerosol-mediated suppression of light precipitation via cloud microphysical
405 feedbacks (Twomey, 1977). Conversely, positive SHAP values (+0.38 to +3.48) correspond to PM_{2.5} reductions (<30 $\mu\text{g m}^{-3}$), reflecting enhanced light rain frequency through improved cloud droplet coalescence efficiency. These findings corroborate XGBoost-derived conclusions, reinforcing the robustness of aerosol-driven mechanisms in light precipitation regulation. The SEM analysis further corroborates aerosols direct suppression effect on light rain frequency, demonstrating a significant
410 negative correlation ($r = -0.29$, $p < 0.01$; Fig. 10). SEM also elucidates indirect pathways through which PM_{2.5} modulates precipitation by altering key meteorological factors. For example, PM_{2.5} exhibits an inverse correlation with total column water vapor (TCLW; $r = -0.23$, $p < 0.05$), indicating aerosol-mediated cloud liquid water reduction (Fig. 10). Mechanistically, elevated aerosols reduce TCLW through two synergistic pathways, firstly, the increased aerosols enhanced cloud droplet evaporation due
415 to radiative heating (the semi-direct effect) (Hansen et al., 1997; Johnson et al., 2004; Huang et al., 2014; Fan et al., 2015); second, Elevated aerosol loading can reduce TCLW by enhancing cloud-top radiative cooling and turbulent entrainment, which introduce dry air into the cloud, promote droplet evaporation, and decrease cloud water content (Wang et al., 2003; Ackerman et al., 2004; Bretherton et al., 2007; Xue et al., 2008; Williams and Igel, 2021; Fons et al., 2023). In addition, increased aerosol concentrations

420 suppress evaporation (E; $r = -0.14$, $p < 0.05$), reflecting radiative cooling effects that reduce atmospheric moisture (Niu et al., 2010). These combined effects diminish liquid water accumulation and cloud droplet growth, ultimately suppressing light precipitation. Furthermore, SEM reveals aerosols-RH coupling interaction ($r = -0.42$, $p < 0.001$), confirming aerosols dual regulatory roles in direct microphysical suppression and indirect climatic feedbacks.



425

Figure 9. The SHAP values of each individual factor to the long-term trends of light rain days in the six selected regions of China.



430 **Figure 10.** SEM to determine the effects of factors on light rain days. The numbers next to the arrows represent normalized path coefficients. All the paths' coefficients in the model were highly significant ($p < 0.001$).

Note that, the SEM analysis demonstrates a significant positive correlation between TCLW and precipitation ($r = 0.41, p < 0.01$) (Fig. 10). While in highly polluted regions (e.g., NC and FW), elevated 435 TCLW values exhibit negative SHAP values, suggesting aerosol-mediated suppression of light precipitation. This inverse relationship may stem from enhanced convective precipitation efficiency under extreme aerosol loading in northern China (Li et al., 2011), where cloud water is preferentially partitioned into precipitation rather than sustaining liquid water accumulation. Conversely, in other regions, TCLW increases correlate positively with light rain frequency, which is in accordance with the results of previous 440 studies (Liu et al., 2011; Wu et al., 2017; Y. Zhang et al., 2019) indicating distinct aerosol thresholds governing cloud microphysical processes. These findings also align with the mechanism proposed by (Zhang et al., 2019). Further analysis reveals that models constructed with warm-season data demonstrate

robust performance (Figs. S12.13), with prediction outcomes exhibiting high consistency with those derived from annual datasets. This finding validates, at a seasonal scale, the cross-seasonal stability of
445 PM_{2.5} concentration impact on light rainfall frequency (Figs. S14 - 17).

In conclusion, our long-term observational analysis (2000 – 2022) reveals a declining trend in light rain occurrences ($-1.0 \text{ days yr}^{-1}$, $p < 0.05$) during 2000–2013, followed by a significant reversal to increasing trends ($+1.9 \text{ days yr}^{-1}$, $p < 0.01$) post - 2013. This decadal shift exhibits an inverse correlation
450 between aerosol loading and light rain frequency across most regions of China, consistent with anthropogenic aerosol impacts on cloud microphysics. Machine learning (XGBoost-SHAP) and SEM jointly demonstrate aerosol's dominant role in driving these trends, with mechanistic insights into cloud droplet coalescence suppression. Meteorological factors (RH, LCC) show non-significant interannual variability ($\Delta < 0.1 \text{ days yr}^{-1}$, $p > 0.1$), indicating negligible contributions to light rain variability over a decade scale. The study reveals dual benefits of China's emission reduction measures on improving air
455 quality and responding to extreme precipitation weather. Despite our model yielding new insights into the aerosols role in affecting the long-term changes of light rainfall in China, there remain uncertainties due to limitations in the model algorithms, variable selection and data resolution. In future work, consideration can be given to incorporating more variables and utilizing different reanalysis datasets to improve the model performance.

460

Data availability. Data are available from the following sites: CPC-global,<https://psl.noaa.gov/data/grid/ded/data.cpc.globalprecip.html>; ERA5,<https://www.ecmwf.int/en/forecasts/dataset/ecmwf-reanalysis-v5>; CHAP, <https://zenodo.org/records/6398971>

Code availability. All code is available upon <https://github.com/TK-0908/>

465 **Declaration of competing interest.** The authors declare no competing interests.

Author contributions. FZ and RZ conceived the conceptual development of the manuscript. LC directed experiments and RZ performed the experiments with PW, GL and XH, and FZ and RZ conducted the data analysis and wrote the draft of the manuscript, and all authors edited and commented on the various sections of the manuscript.

470 **Acknowledgments.** This work was funded by the National Natural Science Foundation of China (NSFC) research project (Grant No. 42475112), Shenzhen Science and Technology Plan Project (Grant No. GXWD20220811174022002; KCXST2022102111404011; [GXWD20220818172959001](https://doi.org/10.5194/acp-18-17295-2018)), Guangdong Natural Science Foundation (Grant No. 2024A1515011005).

References

475 Ackerman, A.S., Kirkpatrick, M.P., Stevens, D.E., Toon, O.B.: The impact of humidity above stratiform clouds on indirect aerosol climate forcing, *Nature*, 432, 1014–1017, <https://doi.org/10.1038/nature03174>, 2004.

IPCC: AR6 Synthesis Report: Climate Change 2023, Intergovernmental Panel on Climate Change, 2023, <https://www.ipcc.ch/report/ar6/syr/>, last access: 5 February 2025.

480 Bai, Y., Liu, M.: Multi-scale spatiotemporal trends and corresponding disparities of PM2.5 exposure in China. *Env. pollution*, 340, 122857. <https://doi.org/10.1016/j.envpol.2023.122857>, 2024.

Bastin, S., Drobinski, P., Chiriaco, M., Bock, O., Roehrig, R., Gallardo, C., Conte, D., Domínguez Alonso, M., Li, L., Lionello, P., Parracho, A.C.: Impact of humidity biases on light precipitation occurrence: observations versus simulations, *Atmos. Chem. Phys.*, 19, 1471–1490, <https://doi.org/10.5194/acp-19-1471-2019>, 2019.

485 Bretherton, C.S., Blossey, P.N., Uchida, J.: Cloud droplet sedimentation, entrainment efficiency, and subtropical stratocumulus albedo, *Geophys. Res. Lett.*, 34, <https://doi.org/10.1029/2006GL027648>, 2007.

Chen, L., Zhang, F., Ren, J., Li, Z., Xu, W., Sun, Y., Liu, L., Wang, X.: Changes in wintertime visibility across China over 2013–2019 and the drivers: A comprehensive assessment using machine learning method. *Sci. Total Environ.*, 912, 169516. <https://doi.org/10.1016/j.scitotenv.2023.169516>, 2024.

490 Chen, T., Guestrin, C.: XGBoost: A Scalable Tree Boosting System, in: *KDD '16: Proceedings of the 22nd ACM SIGKDD International Conference on Knowledge Discovery and Data Mining*, 785–794. <https://doi.org/10.1145/2939672.2939785>, 2016.

Chen, Y., Li, Z., Fan, Y., Wang, H., Fang, G.: Research progress on the impact of climate change on water resources in the arid region of Northwest China, *Acta Geographica Sinica*, 69, 1295–1304, <https://doi.org/10.11821/dlx201409005>, 2014.

495 Cheng, Y., Huang, X., Peng, Y., Tang, M., Zhu, B., Xia, S., He, L.: A novel machine learning method for evaluating the impact of emission sources on ozone formation, *Environ. Pollut.*, 316, 120685, <https://doi.org/10.1016/j.envpol.2022.120685>, 2023.

Cheng, Y., Zhu, Q., Peng, Y., Huang, X., He, L.: Multiple strategies for a novel hybrid forecasting algorithm of ozone based on data-driven models, *J. Cleaner Prod.*, 326, 129451, <https://doi.org/10.1016/j.jclepro.2021.129451>, 2021.

500 Choi, Y., Ho, C., Kim, J., Gong, D., Park, R.J.: The Impact of Aerosols on the Summer Rainfall Frequency in China, *J. Appl. Meteorol. Climatol.*, 47, 1802–1813, <https://doi.org/10.1175/2007JAMC1745.1>, 2008.

Cong, Z., Yang, D., Ni, G.: Does evaporation paradox exist in China?, *Hydrol. Earth Syst. Sci.*, 13, 357–366, <https://doi.org/10.5194/hess-13-357-2009>, 2009.

Dunkerley, D. L.: Light and low-intensity rainfalls: A review of their classification, occurrence, and importance in landsurface, ecological and environmental processes, *Earth-Sci. Rev.*, 214, 103529, <https://doi.org/10.1016/j.earscirev.2021.103529>, 2021.

505 Fan, J., Rosenfeld, D., Yang, Y., Zhao, C., Leung, L. R., Li, Z.: Substantial contribution of anthropogenic air pollution to catastrophic floods in Southwest China: AIR POLLUTION TO CATASTROPHIC FLOODS, *Geophys. Res. Lett.*, 42, 6066–6075, <https://doi.org/10.1002/2015GL064479>, 2015.

510 Fons, E., Runge, J., Neubauer, D., Lohmann, U.: Stratocumulus adjustments to aerosol perturbations disentangled with a causal approach, *npj Clim. Atmos. Sci.*, 6, 130, <https://doi.org/10.1038/s41612-023-00452-w>, 2023.

Fu, C., Dan, L.: Trends in the different grades of precipitation over South China during 1960–2010 and the possible link with anthropogenic aerosols, *Adv. Atmos. Sci.*, 31, 480–491, <https://doi.org/10.1007/s00376-013-2102-7>, 2014.

515 Fu, J., Qian, W., Lin, X., Chen, D.: Trends in graded precipitation in China from 1961 to 2000, *Adv. Atmos. Sci.*, 25, 267–278, <https://doi.org/10.1007/s00376-008-0267-2>, 2008.

Ganjurjav, H., Gornish, E., Hu, G., Wu, J., Wan, Y., Li, Y., Gao, Q.: Phenological changes offset the warming effects on biomass production in an alpine meadow on the Qinghai–Tibetan Plateau, *J. Ecol.*, 109, 1014–1025, <https://doi.org/10.1111/1365-2745.13531>, 2021.

520 Gao, W., Sui, C., Fan, J., Hu, Z., Zhong, L.: A study of cloud microphysics and precipitation over the Tibetan Plateau by radar observations and cloud-resolving model simulations, *J. Geophys. Res. Atmos.*, 121, 13735–13752, <https://doi.org/10.1002/2015JD024196>, 2016.

525 Gui, K., Che, H., Zeng, Z., Wang, Y., Zhai, S., Wang, Z., Luo, M., Zhang, L., Liao, T., Zhao, H., Li, L., Zheng, Y., Zhang, X.: Construction of a virtual PM2.5 observation network in China based on high-density surface meteorological observations using the Extreme Gradient Boosting model, *Environ. Int.*, 141, 105801, <https://doi.org/10.1016/j.envint.2020.105801>, 2020.

Guo, J., Su, T., Chen, D., Wang, J., Li, Z., Lv, Y., Guo, X., Liu, H., Cribb, M., Zhai, P.: Declining Summertime Local-Scale Precipitation Frequency Over China and the United States, 1981–2012: The Disparate Roles of Aerosols, *Geophys. Res. Lett.*, 46, 13281–13289, <https://doi.org/10.1029/2019GL085442>, 2019.

530 Hansen, J., Sato, M., Ruedy, R.: Radiative forcing and climate response, *J. Geophys. Res. Atmos.*, 102, 6831–6864, <https://doi.org/10.1029/96JD03436>, 1997.

Huang, G., Wen, G.: Spatial and temporal variations of light rain events over China and the mid-high latitudes of the Northern Hemisphere, *Chin. Sci. Bull.*, 58, 1402–1411, <https://doi.org/10.1007/s11434-012-5593-1>, 2013.

Huang, J., Wang, T., Wang, W., Li, Z., Yan, H.: Climate effects of dust aerosols over East Asian arid and semiarid regions, *J. Geophys. Res. Atmos.*, 119, 11398–11416, <https://doi.org/10.1002/2014JD021796>, 2014.

535 Jiang, Z., Shen, Y., Ma, T., Zhai, P., Fang, S.: Changes of precipitation intensity spectra in different regions of mainland China during 1961–2006. *J. Meteorol. Res.*, 28, 1085–1098, <https://doi.org/10.1007/s13351-014-3233-1>, 2014.

Johnson, B. T., Shine, K. P., Forster, P. M.: The semi-direct aerosol effect: Impact of absorbing aerosols on marine stratocumulus, *Q. J. R. Meteorol. Soc.*, 130, 1407–1422, <https://doi.org/10.1256/qj.03.61>, 2004.

Lamb, E. G., Mengersen, K. L., Stewart, K. J., Attanayake, U., Siciliano, S. D.: Spatially explicit structural equation modeling, *Ecology*, 95, 2434–2442, <https://doi.org/10.1890/13-1997.1>, 2014.

540 Li, H., Zhou, T., Yu, R.: Analysis of July–August Daily Precipitation Characteristics Variation in Eastern China during 1958–2000, *Chinese J. Atmos. Sci.*, 32, 358–370, <https://doi.org/10.3878/j.issn.1006-9895.2008.02.14>, 2008.

Li, Z., Niu, F., Fan, J., Liu, Y., Rosenfeld, D., Ding, Y.: Long-term impacts of aerosols on the vertical development of clouds and precipitation, *Nat. Geosci.*, 4, 888–894, <https://doi.org/10.1038/ngeo1313>, 2011.

545 Li, Z., Rosenfeld, D., Fan, J.: Aerosols and Their Impact on Radiation, Clouds, Precipitation, and Severe Weather Events, in: Oxford Research Encyclopedia of Environmental Science, Oxford University Press, <https://doi.org/10.1093/acrefore/9780199389414.013.126>, 2017.

Liu, B., Xu, M., Henderson, M.: Where have all the showers gone? Regional declines in light precipitation events in China, 1960-2000, *Int. J. Climatol.*, 31, 1177–1191, <https://doi.org/10.1002/joc.2144>, 2011.

550 Liu, J., Zhao, C., Lin, Y., Zhang, Q., Liu, H., Xiao, Q., Peng, Y.: Potential Impacts of Aerosol on Diurnal Variation of Precipitation in Autumn Over the Sichuan Basin, China, *J. Geophys. Res.-Atmos.*, 127, e2022JD036674, <https://doi.org/10.1029/2022JD036674>, 2022.

555 Lu, E., Zeng, Y., Luo, Y., Ding, Y., Zhao, W., Liu, S., Gong, L., Jiang, Y., Jiang, Z., Chen, H.: Changes of summer precipitation in China: The dominance of frequency and intensity and linkage with changes in moisture and air temperature, *J. Geophys. Res.-Atmos.*, 119, <https://doi.org/10.1002/2014JD022456>, 2014.

Lundberg, S., Lee, S. I.: A Unified Approach to Interpreting Model Predictions, *Adv. Neural Inf. Process. Syst.*, <https://doi.org/10.48550/arXiv.1705.07874>, 2017.

560 Luo, F., Wang, S., Wang, H., Shu, X., Huang, J.: Differing Contributions of Anthropogenic Aerosols and Greenhouse Gases on Precipitation Intensity Percentiles Over the Middle and Lower Reaches of the Yangtze River, *J. Geophys. Res.-Atmos.*, 129, e2023JD040202, <https://doi.org/10.1029/2023JD040202>, 2024.

Ma, S., Zhou, T., Dai, A., Han, Z.: Observed Changes in the Distributions of Daily Precipitation Frequency and Amount over China from 1960 to 2013, *J. Climate*, 28, 6960–6978, <https://doi.org/10.1175/JCLI-D-15-0011.1>, 2015.

565 Ma, W., Ding, J., Wang, J., & Zhang, J.: Effects of aerosol on terrestrial gross primary productivity in Central Asia. *Atmos. Environ.*, 288, 119294. <https://doi.org/10.1016/j.atmosenv.2022.119294>, 2022.

Qian, W., Fu, J., Yan, Z.: Decrease of light rain events in summer associated with a warming environment in China during 1961–2005, *Geophys. Res. Lett.*, 34, <https://doi.org/10.1029/2007GL029631>, 2007.

570 Qian, Y., Gong, D., Fan, J., Leung, L. R., Bennartz, R., Chen, D., Wang, W.: Heavy pollution suppresses light rain in China: Observations and modeling, *J. Geophys. Res.*, 114, D00K02, <https://doi.org/10.1029/2008JD011575>, 2009a.

Qian, Y., Gong, D., Fan, J., Leung, L. R., Bennartz, R., Chen, D., Wang, W.: Heavy pollution suppresses light rain in China: Observations and modeling, *J. Geophys. Res.*, 114, D00K02, <https://doi.org/10.1029/2008JD011575>, 2009b.

Ramanathan, V., Crutzen, P. J., Kiehl, J. T., Rosenfeld, D.: Aerosols, Climate, and the Hydrological Cycle, *Science*, 294, 2119–2124, <https://doi.org/10.1126/science.1064034>, 2001.

Rosenfeld, D., Lohmann, U., Raga, G. B., O'Dowd, C. D., Kulmala, M., Fuzzi, S., Reissell, A., Andreae, M. O.: Flood or Drought: How Do Aerosols Affect Precipitation?, *Science*, 321, 1309–1313, <https://doi.org/10.1126/science.1160606>, 2008.

575 Schreiber, J. B., Nora, A., Stage, F. K., Barlow, E. A., & King, J.: Reporting Structural Equation Modeling and Confirmatory Factor Analysis Results: A Review. *Int. J. Educ. Res.*, 99(6), 323–338. <https://doi.org/10.3200/JOER.99.6.323-338>, 2006.

Shao, T., Liu, Y., Wang, R., Zhu, Q., Tan, Z., Luo, R.: Role of anthropogenic aerosols in affecting different-grade precipitation over eastern China: A case study, *Sci. Total Environ.*, 807, 150886, <https://doi.org/10.1016/j.scitotenv.2021.150886>, 2022.

580 Si, M., Du, K.: Development of a predictive emissions model using a gradient boosting machine learning method, *Environ. Technol. Innov.*, 20, 101028, <https://doi.org/10.1016/j.eti.2020.101028>, 2020.

Song, S., Jing, C., Hu, Z.: Opposite Trends in Light Rain Days over Western and Eastern China from 1960 to 2014, *Atmosphere*, 8, 54, <https://doi.org/10.3390/atmos8030054>, 2017.

585 Trenberth, K. E., Dai, A., Rasmusson, R. M., Parsons, D. B.: The Changing Character of Precipitation, *Bull. Amer. Meteorol. Soc.*, 84, 1205–1218, <https://doi.org/10.1175/BAMS-84-9-1205>, 2003.

Twomey, S.: The Influence of Pollution on the Shortwave Albedo of Clouds, *J. Atmos. Sci.*, 34, 1149–1152, [https://doi.org/10.1175/1520-0469\(1977\)034<1149:TIOPOT>2.0.CO;2](https://doi.org/10.1175/1520-0469(1977)034<1149:TIOPOT>2.0.CO;2), 1977.

590 Wang, S., Wang, Q., Feingold, G.: Turbulence, Condensation, and Liquid Water Transport in Numerically Simulated Nonprecipitating Stratocumulus Clouds, *J. Atmos. Sci.*, 60, 262–278, [https://doi.org/10.1175/1520-0469\(2003\)060<0262:TCALWT>2.0.CO;2](https://doi.org/10.1175/1520-0469(2003)060<0262:TCALWT>2.0.CO;2), 2003.

595 Wang, Y., Ma, P., Jiang, J., Su, H., Rasch, P. J.: Toward reconciling the influence of atmospheric aerosols and greenhouse gases on light precipitation changes in Eastern China, *J. Geophys. Res. Atmos.*, 121, 5878–5887, <https://doi.org/10.1002/2016JD024845>, 2016.

Wang, Y., Shen, X., Jiang, M.: Spatial-Temporal Variation Characteristics of Different Grades of Precipitation in Changbai Mountain from 1961 to 2018, *Clim. Environ. Res.*, 26, 227–238, 2021.

600 Wei, J., Huang, W., Li, Z., Xue, W., Peng, Y., Sun, L., Cribb, M.: Estimating 1-km-resolution PM2.5 concentrations across China using the space-time random forest approach, *Remote Sens. Environ.*, 231, 111221, <https://doi.org/10.1016/j.rse.2019.111221>, 2019.

Wei, J., Li, Z., Lyapustin, A., Sun, L., Peng, Y., Xue, W., Su, T., Cribb, M.: Reconstructing 1-km-resolution high-quality PM2.5 data records from 2000 to 2018 in China: spatiotemporal variations and policy implications, *Remote Sens. Environ.*, 252, 112136, <https://doi.org/10.1016/j.rse.2020.112136>, 2021.

605 Wei, J., Li, Z.: ChinaHighPM2.5: High-resolution and High-quality Ground-level PM2.5 Dataset for China (2000–2023), National Tibetan Plateau Data Center, <https://doi.org/10.5281/zenodo.3539349>, 2024.

Williams, A. S., Igel, A. L.: Cloud Top Radiative Cooling Rate Drives Non-Precipitating Stratiform Cloud Responses to Aerosol Concentration, *Geophys. Res. Lett.*, 48, e2021GL094740, <https://doi.org/10.1029/2021GL094740>, 2021.

610 Wu, J., Ling, C., Zhao, D., Zhao, B.: A counterexample of aerosol suppressing light rain in Southwest China during 1951–2011, *Atmos. Sci. Lett.*, 17, 1–7, <https://doi.org/10.1002/asl.682>, 2016.

Wu, J., Zhang, L., Gao, Y., Zhao, D., Zha, J., Yang, Q.: Impacts of cloud cover on long-term changes in light rain in Eastern China, *Int. J. Climatol.*, 37, 4409–4416, <https://doi.org/10.1002/joc.5095>, 2017.

615 Wu, J., Zhang, L., Zhao, D., Tang, J.: Impacts of warming and water vapor content on the decrease in light rain days during the warm season over eastern China, *Clim. Dyn.*, 45, 1841–1857, <https://doi.org/10.1007/s00382-014-2438-4>, 2015.

Wu, S.: Changing characteristics of precipitation for the contiguous United States, *Clim. Change*, 132, 677–692, <https://doi.org/10.1007/s10584-015-1453-8>, 2015.

620 Xue, H., Feingold, G., Stevens, B.: Aerosol Effects on Clouds, Precipitation, and the Organization of Shallow Cumulus Convection, *J. Atmos. Sci.*, 65, 392–406, <https://doi.org/10.1175/2007JAS2428.1>, 2008.

Yang, X., Zhao, C., Zhou, L., Wang, Y., Liu, X.: Distinct impact of different types of aerosols on surface solar radiation in China, *J. Geophys. Res. Atmos.*, 121, 6459–6471, <https://doi.org/10.1002/2016JD024938>, 2016.

625 Yang, Y., Zhang, C., Zhang, J., Wang, Y.: Changes in soil moisture and dryness and their response to climate change in the Guanzhong region, *Arid Zone Research*, 41, 261–271, <https://doi.org/10.13866/j.azr.2024.02.09>, 2024.

Yuan, Z., Zhang, Z., Yan, J., Liu, J., Hu, Z., Wang, Y., Cai, M.: Spatiotemporal characteristics of different grades of precipitation in Yellow River Basin from 1960 to 2020, *Arid Zone Research*, 41, 1259–1271, <https://doi.org/10.13866/j.azr.2024.08.01>, 2024.

630 Zhang, S., Wu, J., Zhao, D., Xia, L.: Characteristics and reasons for light rain reduction in Southwest China in recent decades, *Prog. Phys. Geogr.*, 43, 643–665, <https://doi.org/10.1177/0309133319861828>, 2019.

Zhang, Y., Liu, C., You, Q., Chen, C., Xie, W., Ye, Z., Li, X., He, Q.: Decrease in light precipitation events in Huai River Eco-economic Corridor, a climate transitional zone in eastern China, *Atmos. Res.*, 226, 240–254, <https://doi.org/10.1016/j.atmosres.2019.04.027>, 2019.

635 Zhang, Z., Wang, K.: Quantifying and adjusting the impact of urbanization on the observed surface wind speed over China from 1985 to 2017, *Fundamental Res.*, 1, 785–791, <https://doi.org/10.1016/j.fmre.2021.09.006>, 2021.

Zhao, C., Tie, X., Lin, Y.: A possible positive feedback of reduction of precipitation and increase in aerosols over eastern central China, *Geophys. Res. Lett.*, 33, <https://doi.org/10.1029/2006GL025959>, 2006.

Zhang, F., Wang, Y., Peng, J., Chen, L., Sun, Y., Duan, L., Ge, X., Li, Y., Zhao, J., Liu, C., Zhang, X., Zhang, G., Pan, Y., 640 Wang, Y., Zhang, A. L., Ji, Y., Wang, G., Hu, M., Molina, M. J., Zhang, R.: An unexpected catalyst dominates formation and radiative forcing of regional haze, *PNAS*, 117(8), 3960–3966, <https://doi.org/10.1073/pnas.1919343117>, 2020.

Zhou, J., Zhi, R., Li, Y., Zhao, J., Xiang, B., Wu, Y., Feng, G.: Possible causes of the significant decrease in the number of summer days with light rain in the east of southwestern China, *Atmos. Res.*, 236, 104804, <https://doi.org/10.1016/j.atmosres.2019.104804>, 2020.

Zhang, R., Zhu, S., Zhang, Z., Zhang, H., Tian, C., Wang, S., Wang, P., Zhang, H.: Long-term variations of air pollutants and public exposure in China during 2000–2020, *Sci. Total Environ.*, 2024, 930. <https://doi.org/10.1016/j.scitotenv.2024.172606>, 2024.